Juvenile hormone differentially regulates two *Grp78* genes encoding protein chaperones required for insect fat body cell homeostasis and vitellogenesis

Received for publication, February 10, 2017, and in revised form, March 27, 2017 Published, Papers in Press, March 29, 2017, DOI 10.1074/jbc.M117.780957

Maowu Luo[‡§], Dong Li[¶], Zhiming Wang[‡], Wei Guo[‡], Le Kang[‡1], and Shutang Zhou[¶2]

From the [‡]State Key Laboratory of Integrated Management of Pest Insects and Rodents, Institute of Zoology, Chinese Academy of Sciences, Beijing 100101, the [¶]State Key laboratory of Cotton Biology, Institute of Plant Stress Biology, School of Life Sciences, Henan University, Kaifeng, Henan 475004, and the [§]University of Chinese Academy of Sciences, Beijing 100049, China

Edited by Xiao-Fan Wang

Juvenile hormone (JH) has a well known role in stimulating insect vitellogenesis (*i.e.* yolk deposition) and oocyte maturation, but the molecular mechanisms of JH action in insect reproduction are unclear. The 78-kDa glucose-regulated protein (Grp78) is a heat shock protein 70-kDa family member and one of the most abundant chaperones in the endoplasmic reticulum (ER) where it helps fold newly synthesized peptides. Because of its prominent role in protein folding, and also ER stress, we hypothesized that *Grp78* might be involved in fat body cell homeostasis and vitellogenesis and a regulatory target of JH. We report here that the migratory locust *Locusta migratoria* possesses two *Grp78* genes that are differentially regulated by JH. We found that *Grp78-1* is regulated by JH through Mcm4/7-dependent DNA replication and polyploidization, whereas *Grp78-2* expression is directly activated by the JH-receptor complex comprising methoprene-tolerant and Taiman proteins. Interestingly, *Grp78-2* expression in the fat body is about 10-fold higher than that of *Grp78-1*. Knockdown of either *Grp78-1* or *Grp78-2* significantly reduced levels of vitellogenin (Vg) protein, accompanied by retarded maturation of oocytes. Depletion of both *Grp78-1* and *Grp78-2* resulted in ER stress and apoptosis in the fat body and in severely defective Vg synthesis and oocyte maturation. These results indicate a crucial role of Grp78 in JH-dependent vitellogenesis and egg production. The presence and differential regulation of two *Grp78* genes in *L. migratoria* likely help accelerate the production of this chaperone in the fat body to facilitate folding of massively synthesized Vg and other proteins.

Juvenile hormone (JH),[3] a sesquiterpenoid secreted by corpora allata, controls many aspects of insect physiology including metamorphosis and reproduction. During the larval stage, JH prevents metamorphosis by modifying the action of 20-hydroxyecdysone at each molting (1, 2). Recent studies have revealed that JH exerts its anti-metamorphic role via its receptor, methoprene-tolerant (Met) (3, 4). Upon JH induction, Met heterodimerizes with Taiman (Tai) to transcriptionally activate *Krüppel homolog 1* (*Kr-h1*) (5–8), which represses the expression of genes coding for Broad-complex and E93 (3, 9–12), the triggers of pupal and adult metamorphosis. At the final larval instar, a very low titer or the absence of JH coupled with a peak of 20-hydroxyecdysone then initiates the larva-pupa or larva-adult transition (1, 2). In adults, JH reappears to stimulate the previtellogenic development, vitellogenesis, and oocyte maturation for reproduction (2, 13–16). Vitellogenesis, the process of yolk protein precursor, vitellogenin (Vg) synthesis in the fat body, secretion into the hemolymph, and uptake by the developing oocytes, is crucial to egg production and later embryonic development (2, 13, 15, 17). JH-dependent vitellogenesis has been reported in many insect species, including the red flour beetle *Tribolium castaneum*, the linden bug *Pyrrhocoris apterus*, the German cockroach *Blattella germanica*, the Pacific beetle cockroach *Diploptera punctata*, and the migratory locust *Locusta migratoria* (2, 13, 15, 17–20). In adult female locusts, synthesis and secretion of proteins by the fat body is increased up to 20-fold during the vitellogenic phase and Vg makes up 60% of the secreted proteins (2, 21). To facilitate massive Vg synthesis, the fat body undergoes JH-dependent build-up of cellular structures such as endoplasmic reticulum (ER) and ribosomes (2). Thus, JH may act on certain genes directly and others through a cascade of effects to maintain cell homeostasis.

The 78-kDa glucose-regulated protein (Grp78), also known as immunoglobulin heavy-chain binding protein (BiP), is a member of heat shock protein 70-kDa family (22, 23). As the most abundant chaperone protein in ER lumens, Grp78 binds to newly synthesized peptides to facilitate them folding (23, 24). Surplus Grp78 interacts with inositol-requiring enzyme-1 (Ire1), protein kinase RNA-like ER kinase (Perk), and activating transcription factor-6 (Atf6) to inhibit their activity (25–28). When the unfolded or misfolded proteins accumulate, ER homeostasis is perturbed to a condition referred to as ER stress (26, 27, 29). Release of Grp78 from the complexes with Ire1, Perk, and Atf6 allows these proteins to be activated by

This work was supported by National Natural Science Foundation of China Grants 31630070 and 31372258. The authors declare that they have no conflicts of interest with the contents of this article.

[1] To whom correspondence may be addressed. E-mail: lkang@ioz.ac.cn.
[2] To whom correspondence may be addressed. Tel.: 86-371-63886272; E-mail address: szhou@henu.edu.cn.

[3] The abbreviations used are: JH, juvenile hormone; Met, methoprene-tolerant; Vg, vitellogenin; ER, endoplasmic reticulum; Grp78, 78-kDa glucose-regulated protein; Ire1, inositol-requiring enzyme-1; Perk, protein kinase RNA-like ER kinase; ATF6, activating transcription factor-6; UPR, unfolded protein response; Mcm, mini-chromosome maintenance; PAE, post-adult eclosion; qRT, quantitative RT; JHA, JH analog; nt, nucleotides(s); Gce, Germ cell-expressed; PDI, protein-disulfide isomerase; eIF2α, eukaryotic initiation factor 2α; Tai, Taiman.

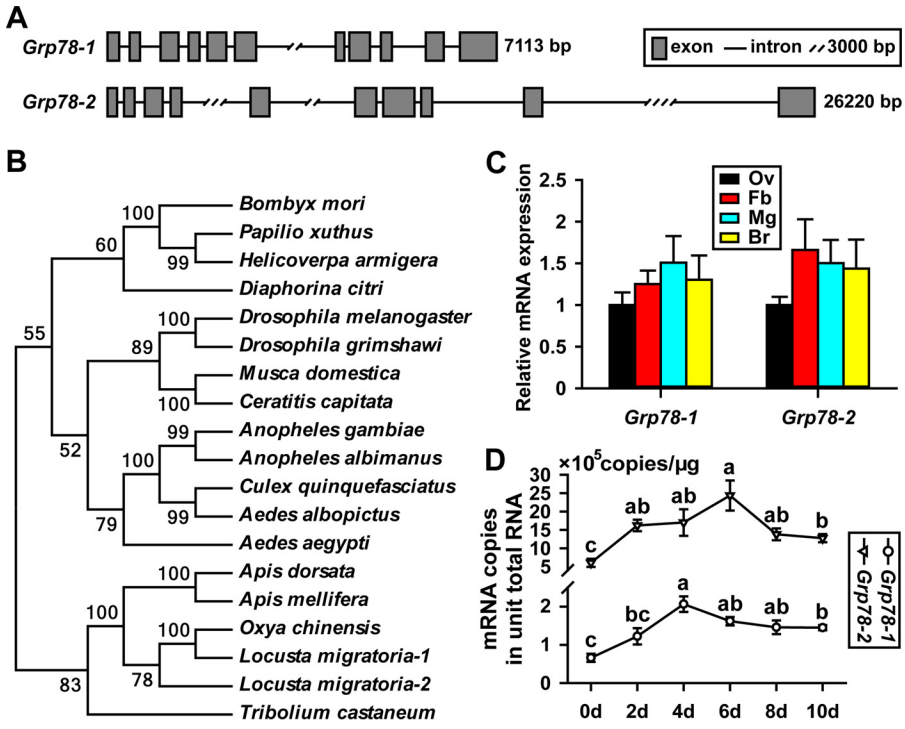

Figure 1. Characteristics of two *Grp78* genes and their expression profiles in *L. migratoria*. *A,* gene structures of locust *Grp78-1* and *Grp78-2*. *B,* the phylogenetic tree constructed with the coding sequences of *Grp78* genes. *Bombyx mori*, silkworm; *Papilio xuthus*, xuthus swallowtail; *Helicoverpa armigera*, cotton bollworm; *Diaphorina citri*, Asian citrus psyllid; *D. melanogaster*, fruit fly; *Drosophila grimshawi*, Hawaiian fruit fly; *Musca domestica*, housefly; *Ceratitis capitata*, mediterranean fruit fly; *Anopheles gambiae*, malaria mosquito; *Anopheles albimanus*, another malaria mosquito; *Culex quinquefasciatus*, Southern house mosquito; *Aedes albopictus*, Asian tiger mosquito; *Aedes aegypti*, yellow fever mosquito; *Apis dorsata*, giant honeybee; *Apis mellifera*, European honeybee; *Oxya chinensis*, rice grasshopper; *L. migratoria*, migratory locust; *T. castaneum*, red flour beetle. *C,* relative expression levels of *Grp78-1* and *Grp78-2* in the selected tissues of adult female locusts at 8 days PAE. *Ov*, ovary; *Fb*, fat body; *Mg*, midgut; *Br*, brain. $n = 12–16$. *D,* absolute quantification of *Grp78-1* and *Grp78-2* mRNA abundance in the fat body of adult females from 0 to 10 days PAE. For each gene, *different letters* indicate significant difference in mRNA abundance between the developmental stages. $p < 0.05$ ($n = 12–16$).

homodimerization and phosphorylation, which triggers the unfolded protein response (UPR) to restore ER homeostasis via enhancing the folding capacity and reducing the protein load in the ER (26–29). When cells undergo severe or prolonged ER stress, apoptosis is induced (25–27, 30). In mammals, Grp78-related ER stress has been reported in obesity (31, 32), type II diabetes (32–34), cholestasis-induced liver injury (35, 36), heart ischemia/reperfusion damage (37), atherosclerotic lesions (38), neurodegenerative diseases (39–41), intestinal inflammation (42, 43), and cancer (44). In insects, studies on this chaperone have been limited to *Drosophila melanogaster*, in which Grp78 (also called heat shock 70-kDa protein cognate 3, Hsc70-3 or Hsc3) links to the ER stress and is involved in the centrosome duplication, regulation of glucose metabolism, RNA interference response, and sleep deprivation (45–48). It has also been reported that Grp78 together with other heat shock proteins contribute to cell preservation over the winter in the goldenrod gall fly *Eurosta solidaginis* (49).

Considering the massive Vg synthesis in the fat body of vitellogenic adult insects, we hypothesized that Grp78 might be involved in fat body cell homeostasis and vitellogenesis. *L. migratoria* has been served as an ideal model to study the JH-dependent vitellogenesis and egg production, as JH controls locust Vg synthesis in the fat body, secretion into the hemolymph, and uptake by the developing oocytes (2, 50–52). Here we report two *Grp78* genes identified in *L. migratoria*. We found that *Grp78-1* is regulated by JH via mini-chromosome maintenance protein (Mcm) 4- and 7-mediated DNA replication, whereas *Grp78-2* is directly activated by the JH-receptor complex. We demonstrated that knockdown of either *Grp78-1* or *Grp78-2* can cause a significant reduction of Vg levels and the impaired oocyte maturation. However, depletion of both *Grp78* genes results in more defective phenotypes along with ER stress and apoptosis in the fat body, which restrains the response of locusts to exogenous application of JH. These results provide new insights into the mechanisms of JH regulation in insect reproduction.

Results

Two Grp78 genes are identified in the migratory locust

The sequenced locust genome (53) yielded two *Grp78* genes, *Grp78-1* (GenBank™ FJ472842) and *Grp78-2* (GenBank™ FJ472843). The *Grp78-1* gene is 7,113 bp comprised of 11 exons, whereas the *Grp78-2* gene is 26,220 bp with 10 exons (Fig. 1*A*). *Grp78-1* and *Grp78-2* cDNA are 2,395 and 2,583 bp, respectively, and their proteins share 87% identity of amino acids. Phylogenetic tree construction revealed that *Grp78* genes are evolutionally conserved, and locust *Grp78-1* is closer to *Grp78* of the rice grasshopper *Oxya chinensis* (Fig. 1*B*). Intriguingly, a single *Grp78* gene is reported in other insect species available in the databases including NCBI, FlyBase, and VectorBase. The presence of two *Grp78* genes in *L. migratoria* might

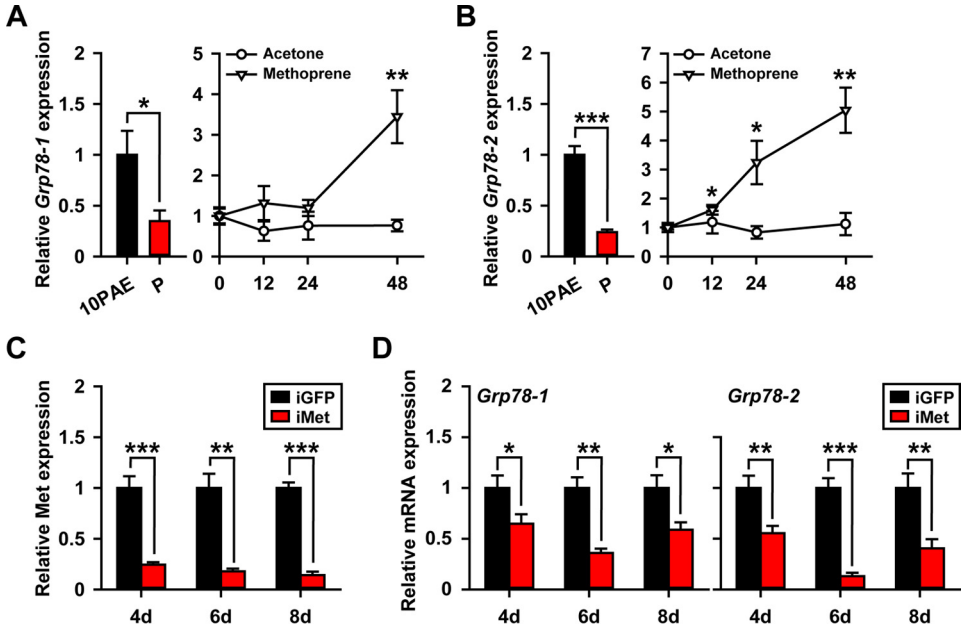

Figure 2. Responsiveness of *Grp78-1* and *Grp78-2* to JH and Met. *A* and *B*, relative mRNA levels of *Grp78-1* (*A*) and *Grp78-2* (*B*) in the fat body of adult females treated with precocene for 10 days (*P*) and those further treated with methoprene or acetone (solvent control) for 12–48 h. *PAE10*, 10-day-old adult females as the positive control. *, $p < 0.05$ and **, $p < 0.01$ ($n = 8$). *C*, *Met* knockdown efficiency in the fat body of dsMet-injected adult females (iMet) at 4–8 days PAE. **, $p < 0.01$ and ***, $p < 0.001$ compared with the respective dsGFP controls (iGFP) ($n = 8$). *D*, effect of *Met* RNAi on the expression of *Grp78-1* and *Grp78-2* in the fat body on day 4–8. *, $p < 0.05$; **, $p < 0.01$; and ***, $p < 0.001$ compared with the respective dsGFP controls ($n = 8$).

reflect an evolutional gene duplicate in this primitive insect species.

The first gonadotrophic cycle of adult female locusts was ~11 days and vitellogenesis started from ~5 days post-adult eclosion (PAE). To explore the spatial expression patterns of two *Grp78* genes in locusts, qRT-PCR was conducted using total RNA from the fat body (Fb), ovary (Ov), midgut (Md), and brain (Br) of adult females collected at 8 days PAE. As shown in Fig. 1*C*, *Grp78-1* and *Grp78-2* were expressed at similar levels in these selected tissues. As the fat body is the primary tissue for protein synthesis during vitellogenesis, we next performed absolute quantitative RT-PCR to compare the transcript levels of *Grp78-1* and *Grp78-2* in the fat body of adult females from 0 (the day of eclosion) to 10 days PAE. For developmental profiles, *Grp78-1* mRNA levels in the fat body were significantly increased by 3.1-fold at 4 days PAE compared with that at 0 day PAE, then declined but remained significantly elevated (2.2–2.5-fold) on days 6–10 (Fig. 1*D*). With respect to *Grp78-2*, its transcript levels were significantly increased by 2.8-fold at 2 days PAE, and remained high (2.2–4.0-fold) on days 4–10 (Fig. 1*D*). As locust hemolymph JH titer is undetectable at eclosion but elevates significantly in the previtellogenic stage and rises to a peak during vitellogenesis (54, 55), the increase of *Grp78* mRNA levels appeared to correlate with the phase of increased JH titers. Although *Grp78-1* and *Grp78-2* had similar expression patterns from 0 to 10 days PAE, 1 μg of total RNA of fat bodies appeared to have $0.7–2.1 \times 10^5$ copies of *Grp78-1* mRNA and $6.0–24.4 \times 10^5$ copies of *Grp78-2* mRNA, respectively (Fig. 1*D*). The data indicate that the abundance of *Grp78-2* mRNA was about 10-fold higher than that of *Grp78-1*.

Grp78-1 and Grp78-2 are expressed in response to JH and Met

To evaluate the responsiveness of *Grp78* to JH, qRT-PCR was carried out using total RNA from the fat body of precocene-treated adult females for 10 days as well as those further treated with an active JH analog (JHA), methoprene for 12–48 h. Deprivation of endogenous JH by ablation of corpora allata with precocene treatment caused 65 and 76% reduction of *Grp78-1* and *Grp78-2* mRNA levels, respectively (Fig. 2, *A* and *B*). Further application of methoprene led to a 3.5-fold increase of *Grp78-1* mRNA levels at 48 h (Fig. 2*A*). Interestingly, *Grp78-2* mRNA levels were significantly increased by 1.6-fold at 12 h post-methoprene treatment, and continually elevated by 3.2-fold at 24 h and 5.0-fold at 48 h (Fig. 2*B*), suggesting an earlier responsiveness of *Grp78-2* to JHA. In the parallel experiment of solvent controls, acetone treatment had no significant effect on *Grp78* expression (Fig. 2, *A* and *B*). We next performed *Met* RNAi to assess the requirement of JH receptor for the JH-dependent expression of *Grp78-1* and *Grp78-2*. qRT-PCR demonstrated that 76–86% of *Met* knockdown efficiency was achieved in the fat body of dsMet-injected (iMet) adult females at 4–8 days PAE (Fig. 2*C*). When *Met* was silenced, the mRNA levels of *Grp78-1* and *Grp78-2* were reduced by 35–64 and 45–87%, respectively, on days 4–8 (Fig. 2*D*). Taken together, these data suggest that the expression of *Grp78-1* and *Grp78-2* are in response to JH and its receptor, Met.

Differential regulation of Grp78-1 and Grp78-2 by JH

Previously, the core E-box and E-box-like motifs with variable nucleotides at their flanking regions has been reported as the JH response elements recognized by Met (6, 14, 50, 51, 56–58). We therefore analyzed the 3-kb upstream sequences of both *Grp78-1* and *Grp78-2* genes. An E-box-like motif

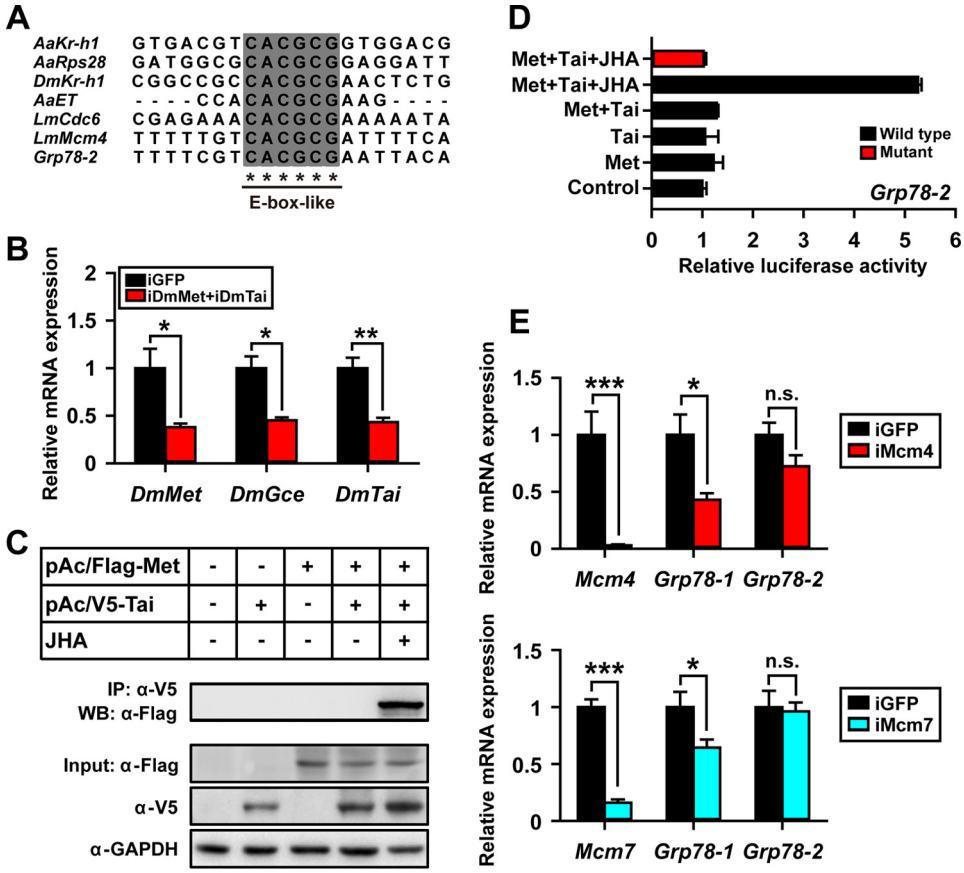

Figure 3. Differential regulation of *Grp78-1* and *Grp78-2* by JH. *A,* alignment of DNA sequences containing E-box-like motif in the promoters of *Kr-h1*, *ribosomal protein S28* (*Rps28*), and *Early trypsin* (*ET*) from the mosquito *A. aegypti* (*Aa*), *Kr-h1* from *D. melanogaster* (*Dm*), as well as *cell-division-cycle 6* (*Cdc6*), *Mcm4,* and *Grp78-2* from the migratory locust *L. migratoria* (*Lm*) (14, 50, 51, 56, 57, 88). *B,* relative expression levels of *DmMet*, *DmGce*, and *DmTai* in S2 cells treated with *Drosophila Met* and *Tai* dsRNA (*iDmMet*+*iDmTai*). *, $p < 0.05$; **, $p < 0.01$ compared with the iGFP control ($n = 3$). *C,* Western blot analysis (*WB*) and immunoprecipitation (*IP*) showing the expression of FLAG-Met (pAc5.1/Flag-Met(1–3108)) and V5-Tai (pAc5.1/V5-Tai(1–1785 plus 4581–4961); Tai-A variant with the INDEL-1/PRD motif) in S2 cells, and the heterodimerization of FLAG-Met and V5-Tai in the presence of methoprene (JHA). *α-FLAG*, anti-FLAG antibody; *α-V5*, anti-V5 antibody; *α-GAPDH*, anti-GAPDH antibody. *D,* luciferase reporter assays using S2 cells pGL4.10/*Grp78-2*(−2068 to −24) + pAc5.1 empty vector (control), co-transfected pGL4.10/*Grp78-2*(−2068 to −24) + pAc5.1/Flag-Met(1–3108) (*Met*), pGL4.10/*Grp78-2*(−2068 to −24) + pAc5.1/V5-Tai(1–1785 plus 4581–4961) (*Tai*), and pGL4.10/*Grp78-2*(−2068 to −24) + pAc5.1/Flag-Met(1–3108) + V5-Tai(1–1785 plus 4581–4961) (*Met*+*Tai*). *Tai*, Tai-A variant with the INDEL-1/PRD motif; *JHA*, methoprene (10 μM); *wild type*, pGL4.10/*Grp78-2*(−2068 to −24) with E-box-like motif; *Mutant*, the pGL4.10/*Grp78-2*(−2068 to −24) in which the E-box like motif (CACGCG) is substituted by the sequence ACATAT. *E,* effect of *Mcm4* RNAi (iMcm4) or *Mcm7* RNAi (iMcm7) on *Grp78-1* and *Grp78-2* expression in the fat bodies of 6-day-old adult females. *, $p < 0.05$; ***, $p < 0.001$; *n.s.*, no significant difference compared with the respective iGFP controls ($n = 8$).

(CACGCG; nt −1661 to −1656) was identified in the promoter of *Grp78-2* (Fig. 3*A*). However, neither E-box nor the E-box-like motif were found in the 3-kb upstream of *Grp78-1*. Interestingly, the flanking regions of E-box-like motif of *Grp78-2* share high nucleotide identity to that of locust *Mcm4* (Fig. 3*A*), which has been experimentally demonstrated for binding by the JH-receptor complex (50). To determine whether the JH-receptor directly activates the transcription of *Grp78-2*, we performed luciferase assays using S2 cells co-transfected with the wild-type or mutational pGL4.10-*Grp78-2*(−2068 to −24) plus pAc5.1/Flag-Met(1–3108) and/or pAc5.1/V5-Tai(1–1785 plus 4581–4961). It must be noted that this Tai variant is Tai-A isoform with the INDEL-1/PRD motif (52). In *Drosophila*, Met has a paralogue, Germ cell-expressed (Gce; FlyBase: FBpp0292296), which shares about 40% identity of amino acids (59, 60). To diminish the interference of endogenous Met, Gce, and Tai, S2 cells were treated with dsRNA of *Drosophila Met* and *Tai* (iDmMet + iDmTai) prior to transfection of the recombinant constructs. As shown in Fig. 3*B*, the mRNA levels of *Drosophila Met*, *Gce*, and *Tai* were reduced by 62, 55, and 57%, respectively (Fig. 3*B*). Immunoprecipitation and Western blot analysis demonstrated that the expressed FLAG-Met and V5-Tai were dimerized in the presence of methoprene (Fig. 3*C*). JHA-induced dimerization of FLAG-Met and V5-Tai led to a 4-fold increase of wild-type *Grp78-2* reporter activity without increase of the E-box-like motif mutant compared with the JHA-untreated group (Fig. 3*D*). These data suggest that the transcription of *Grp78-2* is activated by the JH-receptor complex.

In an earlier report (50), we have demonstrated that the JH-receptor acts on *Mcm4* and *Mcm7* to promote DNA replication and polyploidy for the massive Vg synthesis. We reasoned that *Grp78-1* might be regulated by JH and Met via Mcm4 and Mcm7. To investigate the dependence of *Grp78-1* expression on Mcm4 and Mcm7, we performed RNAi of *Mcm4* (iMcm4) and *Mcm7* (iMcm7) using the fat body from 6-day-old adult females. qRT-PCR showed that 97 and 84% knockdown efficiency were obtained for *Mcm4* and *Mcm7* (Fig. 3*E*), respec-

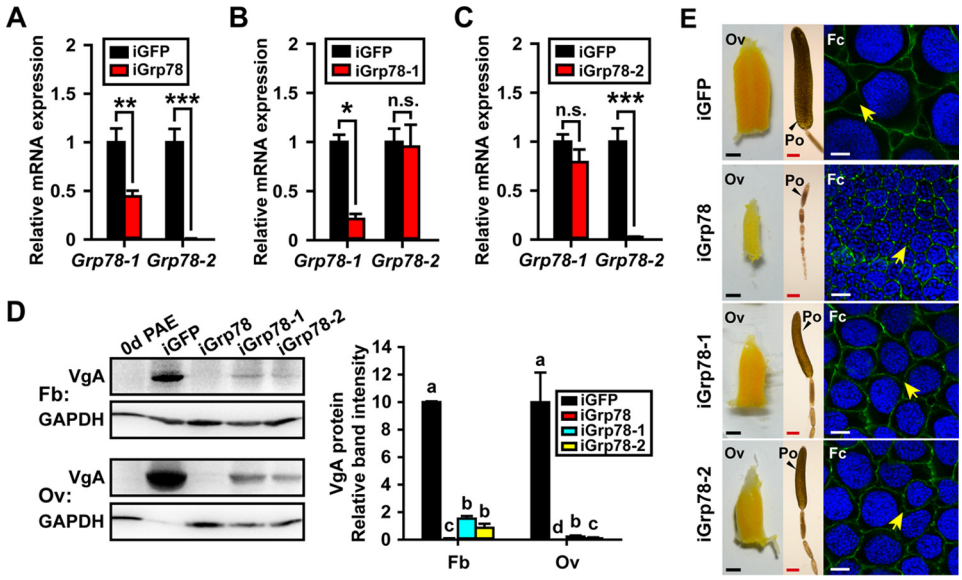

Figure 4. Effects of *Grp78* depletion on vitellogenesis and oocyte maturation. *A–C,* RNAi efficiency of *Grp78-1* and *Grp78-2* in the fat body of 6-day-old adult females treated with dsRNA shared by both *Grp78-1* and *Grp78-2* (iGrp78) (*A*), *Grp78-1*-sepecific dsRNA (iGrp78-1) (*B*), or *Grp78-2*-specific dsRNA (iGrp78-2) (*C*). *, $p < 0.5$; **, $p < 0.01$; ***, $p < 0.001$; *n.s.*, no significant difference ($n = 6–8$). *D,* Western blot analysis (*left panel*) and the quantitative analysis of band intensity by ImageJ (*right panel*) on VgA in the fat body and ovary after iGrp78, iGrp78-1, or iGrp78-2. *0d PAE*, the adult females at day of eclosion was used as a negative control. *Different letters* indicate significant difference at $p < 0.05$ ($n = 3$). *E,* morphology changes of ovaries (*Ov*), primary oocytes (*Po*), and follicle cells (*Fc*) after iGrp78, iGrp78-1, or iGrp78-2 at 6 days PAE. *Scale bar*: *Ov*, 2.5 mm; *Po*, 500 μm; *Fc*, 10 μm. *Blue*, follicle cell nuclei; *green*, F-actin. *Yellow arrows* indicate the patency.

tively. Depletion of *Mcm4* caused 57% reduction of *Grp78-1* mRNA levels, and *Mcm7* knockdown reduced *Grp78-1* abundance to 64% (Fig. 3*E*). However, neither *Mcm4* nor *Mcm7* knockdown inhibited *Grp78-2* expression (Fig. 3*E*). The data suggest that JH acts on *Grp78-1* through Mcm4/7-promoted DNA replication and polyploidization.

Grp78 knockdown suppresses locust vitellogenesis and oocyte maturation

To evaluate the function of Grp78 in JH-mediated vitellogenesis and oocyte maturation, we conducted RNAi via injection of dsRNA shared by both *Grp78-1* and *Grp78-2* (iGrp78), *Grp78-1*-specific dsRNA (iGrp78-1), or *Grp78-2*-specific dsRNA (iGrp78-2). As shown in Fig. 4*A*, iGrp78 gave rise to 56 and 99% reduction of *Grp78-1* and *Grp78-2* expression, respectively, at 6 days PAE. iGrp78-1 caused 87% reduction of *Grp78-1* abundance, but had no significant effect on *Grp78-2* expression (Fig. 4*B*). iGrp78-2 only significantly reduced the expression of *Grp78-2*, with 98% knockdown efficiency (Fig. 4*C*). The migratory locust has two coordinately expressed *Vg* genes, *VgA* (GenBank™ KF171066) and *VgB* (GenBank™ KX709496) that are expressed in similar patterns (50, 51). *VgA* was selected as a representative. Western blot analysis and subsequent quantification of band intensity demonstrated that depletion of both *Grp78-1* and *Grp78-2* caused 99.1 and 99.9% reduction of VgA protein levels in the fat body and ovary, respectively (Fig. 4*D*). When *Grp78-1* was knocked down alone, VgA protein levels were decreased by 84.6% in the fat body and 97.8% in the ovary (Fig. 4*D*). *Grp78-2* RNAi reduced VgA proteins to 7.8 and 1.1% of the control levels in the fat body and ovary, respectively (Fig. 4*D*).

We next examined the phenotypes of *Grp78* knockdown on oocyte maturation and ovarian development. Knockdown of both *Grp78-1* and *Grp78-2* resulted in blocked maturation of primary oocytes and arrested development of ovaries in all experimental locusts. Consequently, the primary oocytes and ovaries of *Grp78*-depleted adult females remained small on day 6 (Fig. 4*E*). In contrast, the primary oocytes and ovaries of iGFP controls were markedly enlarged (Fig. 4*E*). We measured the length of primary oocyte as an indicator of oocyte growth and maturation. Statistically, the length of primary oocytes of iGrp78 locusts was 0.9 mm, whereas that of iGFP controls was 3.7 mm. The defective phenotypes were also observed in adult females subjected to either *Grp78-1* or *Grp78-2* RNAi, but it was less severe than that of *Grp78* RNAi. About 63% of iGrp78-1 and 75% of iGrp78-2 individuals showed significantly impaired oocyte maturation and ovarian growth. As the follicular epithelium determines the size of ovarian follicle and facilitates the transport Vg from the hemolymph to the developing oocytes via the intercellular spaces, known as patency (2, 61), we further examined the morphological change of follicular epithelium after *Grp78* RNAi. Silencing of *Grp78* led to significantly smaller follicle cells and nuclei as well as reduced incidence of patency in comparison with the iGFP controls (Fig. 4*E*). When *Grp78-1* and *Grp78-2* were separately knocked down, the follicle cells and nuclei became slightly smaller, and the patency was also relatively less observed (Fig. 4*E*).

Because locust vitellogenesis and oocyte maturation strictly depend on JH, we next treated *Grp78* RNAi locusts with methoprene to examine whether the defective oocyte maturation, follicular epithelium development, and ovarian growth could be rescued. After methoprene treatment, the expression of neither *Grp78-1* nor *Grp78-2* was significantly increased (Fig. 5, *A* and *B*). As shown in Fig. 5*C*, additional administration of metho-

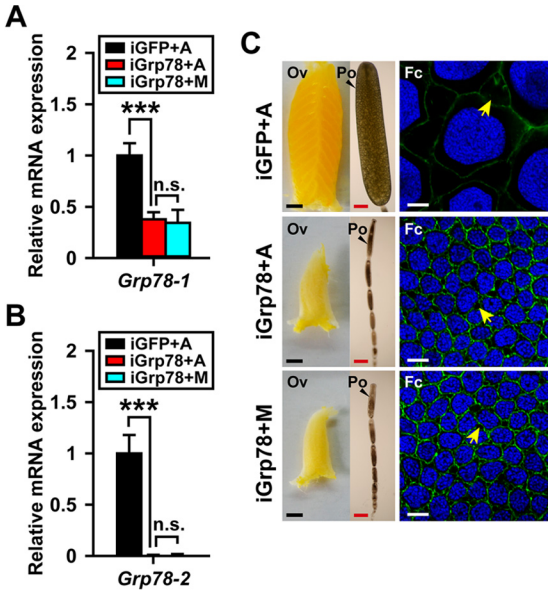

Figure 5. Methoprene treatment fails to rescue the defective phenotypes caused by *Grp78* RNAi. GFP dsRNA (iGFP) or *Grp78* dsRNA (iGrp78) was injected within 12 h post-adult eclosion and boosted on day 5. Methoprene (M) or acetone (A) was applied on day 6, and the effects were examined on day 8. *A* and *B,* the relative expression of *Grp78-1* and *Grp78-2* in the fat body. ***, $p < 0.001$; n.s., no significant difference ($n = 8$). *C,* comparison of ovaries (*Ov*), primary oocytes (*Po*), and follicle cells (*Fc*) of three groups. Scale bar: *Ov*, 2.5 mm; *Po*, 500 μm; *Fc*, 10 μm. *Blue*, follicle cell nuclei; *green*, F-actin. *Yellow arrows* indicate the patency.

prene on *Grp78*-depleted locusts did not restore the defective phenotypes of *Grp78*-depleted locusts to the normal levels. Taken together, these observations indicate that Grp78 plays a critical role in JH-stimulated vitellogenesis and oocyte maturation in locusts.

Grp78 depletion disturbs the homeostasis of fat body cells

The chaperons including the 94-kDa glucose-regulated protein (Grp94, GenBank™ FJ472841), protein-disulfide isomerase (PDI, GenBank™ KX683312), 170-kDa glucose-regulated protein (Grp170, GenBank™ KX683313), and Grp78 have been used as the markers of ER stress because of their transcriptional up-regulation at the early stage of ER stress response (27, 62–66). When Grp78 was knocked down in the fat body (43–66 and 95–99% efficiency for *Grp78-1* and *Grp78-2*, respectively; Fig. 6*A*), the levels of *Grp94* and *PDI* mRNA were increased by 2.2- and 1.8-fold, respectively, at 2 days PAE, whereas *Grp170* mRNA levels was significantly increased by 1.6–2.4-fold at 2–6 days PAE (Fig. 6*B*). As *Grp94*, *PDI*, and *Grp170* are transcriptionally regulated by the Ire1 (GenBank™ KX683314) pathway in the UPR (26, 44, 65–71), we conducted double knockdown by injecting the dsRNA mixture of *Grp78* and *Ire1* (iGrp78 + iIre1) and examined the effects at 6 days PAE. In the iGrp78 + iIre1 group, *Grp94*, *PDI,* and *Grp170* mRNA levels were significantly reduced by 71, 59, and 62%, respectively, compared with the iGrp78 group (Fig. 6*C*). In parallel experiments, depletion of *Ire1* alone (89% knockdown efficiency) did not alter the expression of *Grp78-1*, *Grp78-2*, *Grp94*, *PDI*, *Grp170*, or *VgA* (Fig. 6*D*). Taken together, these data indicate the presence of ER stress in the *Grp78*-depleted fat body and the involvement of Ire1 in the induction of UPR by *Grp78* depletion. To examine the possible apoptosis in the fat body cells caused by *Grp78* depletion, we performed TUNEL assays using adult female locusts treated with dsGrp78 at 6 days PAE. As shown in Fig. 6*E*, apoptotic nuclei were apparently detectable in *Grp78*-depleted fat body cells, indicating an important role of Grp78 in the maintenance of fat body cell homeostasis.

Discussion

Grp78 and JH-stimulated vitellogenesis and oocyte maturation

Using the migratory locust, we demonstrated in this study that loss of *Grp78* function resulted in substantial reduction of Vg, accompanied with arrested oocyte maturation and ovarian growth. Further treatment of the JH analog on *Grp78*-depleted locusts failed to restore the defective phenotypes to the normal levels. These data provide the evidence that Grp78 is essential for JH-stimulated vitellogenesis and egg production. The maturation of pre-vitellogenic adult insects is characterized by the enhanced protein synthesis in the fat body required for oocyte maturation and successful reproduction (2, 13). The secretory proteins like Vg are synthesized, modified, and folded in the ER. It has been documented that Grp78 in the ER lumens functions as a chaperone to facilitate protein folding and to inhibit protein aggregation (27, 29, 30). Grp78 also binds to ER stress sensor proteins including Ire1, Perk, and Atf6 to prevent the activation of UPR (27, 29, 30). In addition, Grp78 binds to Ca^{2+} in the ER and maintains ER Ca^{2+} homeostasis (71, 72). Previous studies have shown that reduction of Grp78 expression in mammalian cells activates UPR and ER stress leading to apoptosis, whereas overexpression of Grp78 protects against ER stress-induced apoptosis (73–77).

In the present study, knockdown of *Grp78* via RNAi in adult female locusts led to ER stress and apoptosis in the fat body. It is likely that loss of Grp78 leads to the accumulation of unfolded or misfolded proteins including Vg, which are transported into cytoplasm to be degraded by proteasome, known as the process of ER-associated degradation (26, 27, 78, 79). It is also likely that depletion of *Grp78* gives rise to activation of Ire1 and Perk. Consequently, Perk phosphorylates eukaryotic initiation factor 2α (eIF2α) to attenuate protein translation globally (80), whereas Ire1 degrades mRNAs in the ER through its RNase activity known as regulated Ire1-dependent decay of mRNA (39). As a consequence, *Grp78*-depleted fat bodies had significantly declined Vg, as well as other regulatory proteins that directly or indirectly regulate Vg synthesis. The locust ovary is panoistic. Vg and other forms of yolk precursor synthesized in the fat body are released into hemolymph and transported to maturing oocytes through the patency in the follicular epithelium (2, 13). The reduced yolk protein precursor production from *Grp78*-depleted fat bodies might consequently result in arrested oocyte maturation and ovarian growth. We also demonstrated that silencing of *Grp78* resulted in smaller follicle cells and nuclei. The follicular epithelium became shrunk and the incidence of patency was reduced. The blocked development of follicular epithelium might alternatively limit the uptake of Vg by the ovary.

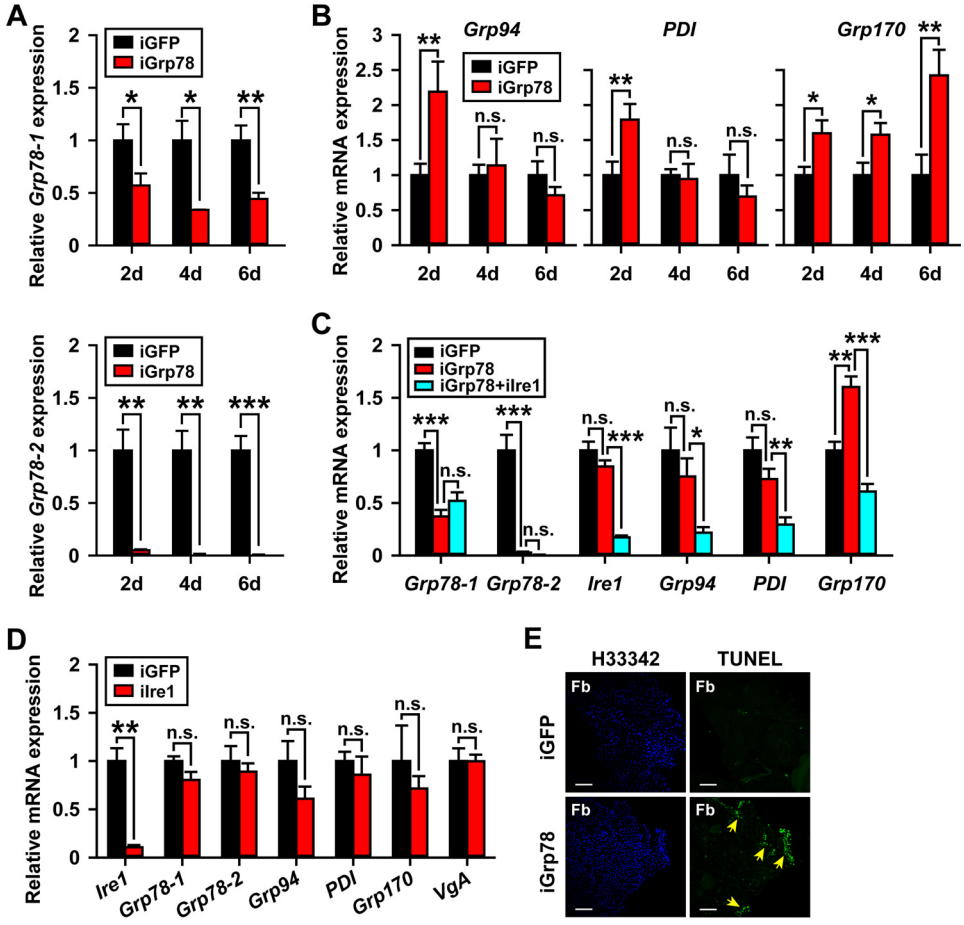

Figure 6. Grp78 knockdown induces fat body cell ER stress and apoptosis. *A,* RNAi efficiency of *Grp78-1* and *Grp78-2* in the fat body of 2–6-day-old adult females treated with dsRNA shared by both *Grp78-1* and *Grp78-2* (iGrp78). *iGFP*, dsGFP control; *, $p < 0.5$; **, $p < 0.01$; ***, $p < 0.001$ ($n = 6–8$). *B,* the relative expression of *Grp94*, *PDI*, and *Grp170* in the fat body of *Grp78*-depleted (iGrp78) adult females at 2–6 days PAE. *iGFP*, dsGFP control; *, $p < 0.05$, **, $p < 0.01$; *n.s.*, no significant difference ($n = 6–8$). *C*, relative expression of *Grp78-1*, *Grp78-2*, *Ire1*, *Grp94*, *PDI*, and *Grp170* in the fat body of adult females in three groups at 6 days PAE. *iGFP*, dsGFP control; *iGrp78*, dsGrp78-injected group; *iGrp78+ilre1*, dsGrp78- and dsIre1-injected group. *, $p < 0.5$; **, $p < 0.01$; ***, $p < 0.001$; *n.s.*, no significant difference ($n = 8$). *D,* the relative mRNA levels of *Ire1*, *Grp78-1*, *Grp78-2*, *Grp94*, *PDI*, *Grp170*, and *VgA* in iGFP *versus* ilre1 groups. **, $p < 0.01$; *n.s.*, no significant difference ($n = 8$). *E,* apoptotic cell detection in *Grp78*-depleted (*iGrp78*) fat body (*Fb*) cells. *H33342*, Hoechst 33342 for staining of nuclei (*blue*); TUNEL, detection of apoptotic cells (*green*), highlighted by *yellow arrows*. *Scale bar*, 200 μm.

Differential regulation of Grp78 genes by JH

Different from a single *Grp78* gene in other insect species whose genome sequences are available in the public databases, two *Grp78* genes were identified in the migratory locust. The genome size of migratory locust is about 6.5 Gb, which is characterized by a large number of repeated sequences (53). Phylogenetic tree construction suggests that *Grp78-2* is likely a new gene evolutionally derived from the locust genome. Our qRT-PCR showed that the expression of both *Grp78-1* and *Grp78-2* was significantly increased in the fat body during the vitellogenic phase, which was in accord with the high levels of JH titer in this stage (54, 55). Notably, the mRNA levels of *Grp78-1* and *Grp78-2* were significantly reduced in adult females chemically allatectomized with precocene treatment, whereas further administration of JH analog induced their expression. Moreover, *Met* RNAi resulted in a significant decrease of *Grp78-1* and *Grp78-2* expression. These results together suggest that the expression of *Grp78-1* and *Grp78-2* is dependent on JH and Met in the fat body of adult female locusts.

Interestingly, the mRNA levels of *Grp78-2* were about 10-fold higher than that of *Grp78-1*. Furthermore, *Grp78-2* expression was significantly increased at 12 h post-JHA treatment, whereas significant induction of *Grp78-1* expression was observed at 48 h. The delayed response of *Grp78-1* to JHA treatment suggests the requirement of additional protein synthesis for *Grp78-1* transcription. Analysis of 3-kb upstream sequences of *Grp78-1* and *Grp78-2* revealed that only the *Grp78-2* promoter possesses a JH response element (E-box-like motif) recognized by the JH-receptor. Given the marked differences in these two genes, it might have been predicted that the JH-receptor directly regulates *Grp78-2* but not *Grp78-1*. This hypothesis is supported by our luciferase reporter assays that demonstrated the activation of *Grp78-2* transcription by Met/Tai in the presence of JHA. During locust vitellogenesis, JH induces extensive DNA replication to produce up to 16-ploid cells in the fat body for massive Vg synthesis (81, 82). Our previous report (50) has demonstrated that the JH-receptor complex acts on *Mcm4* and *Mcm7* for DNA replication and ployploidization. In this study, RNAi and qRT-PCR showed that *Grp78-1* expression was significantly reduced in *Mcm4*- or *Mcm7*-depleted adult females, suggesting that *Grp78-1* is regulated by the JH-Met-Mcm4/7 pathway. It has been reported

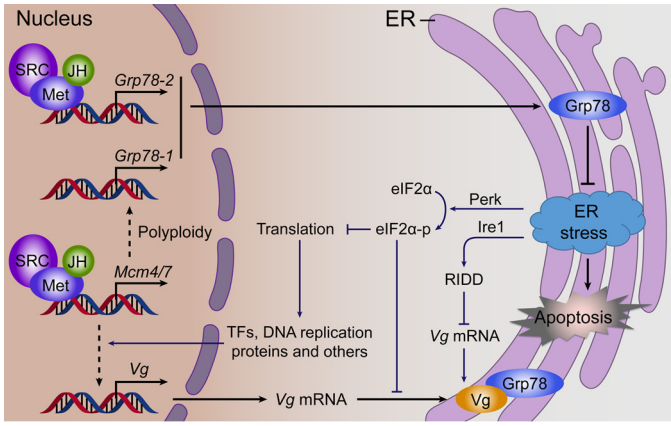

Figure 7. A proposed model for the regulation and function of two *Grp78* genes in JH-stimulated locust vitellogenesis. *Grp78-1* is regulated by the JH-Met-Mcm4/7 pathway, whereas *Grp78-2* is directly activated by the JH-receptor complex. The large amount of Grp78 in the ER facilitates the folding of massively synthesized Vg and other proteins and maintains cell homeostasis. Loss of *Grp78* function induces ER stress, which activates the Ire1-dependent decay (*RIDD*) of mRNA and Perk-eIF2α pathway. RIDD results in the degradation of *Vg* mRNA. The activated eIF2α inhibits protein translation, leading to reduced synthesis of Vg and other regulatory proteins that directly or indirectly regulate Vg synthesis. Consequently, Vg in the fat body and ovary are substantially reduced, and the oocyte maturation and egg production are blocked.

that *Grp78* is transcriptionally regulated by Atf6 and Ire1-activated X-box binding protein 1 (Xbp1) during the UPR through an ER stress-dependent manner (28). *Grp78* is also regulated by insulin-like growth factor-1, Leptin, and miR-376a (83–86). Our data thus extends the view in *Grp78* regulation by demonstrating the differential regulation of two *Grp78* genes in locusts.

Although knockdown of *Grp78-1* or *Grp78-2* suppressed locust vitellogenesis and oocyte maturation, loss of both *Grp78-1* and *Grp78-2* function resulted in much severer defects. These observations address the importance of both *Grp78-1* and *Grp78-2* in JH-dependent female locust reproduction. An adult female locust possesses a pair of ovaries made up of approximately a total of 80 ovarioles. Our study suggests that the migratory locust has adapted a mechanism with two differentially regulated *Grp78* genes to facilitate the proper folding of massively synthesized Vg and other proteins, and to protect fat body cells from possible ER stress during vitellogenesis. The direct activation of *Grp78-2* by the JH-receptor appears to be a more efficient production of this chaperone protein. On the basis of our findings, we propose a model for the regulation and function of locust *Grp78-1* and *Grp78-2* in JH-stimulated vitellogenesis and oocyte maturation (Fig. 7). During insect vitellogenesis, JH acts via its receptor to directly activate the transcription of *Grp78-2*, while up-regulating *Grp78-1* expression through the Met-Mcm4/7 pathway. Grp78 in the ER binds to newly synthesized Vg and other proteins to facilitate their folding and maintain cell homeostasis. Lack of Grp78 induces ER stress and UPR, consequently activating the ER-associated degradation of unfolded proteins including Vg, the Ire1-dependent decay of mRNA (RIDD) including *Vg* mRNA, and the Perk-eIF2α pathway. The phosphorylated eIF2α attenuates translation globally, leading to reduced synthesis of Vg as well as other regulatory proteins that directly or indirectly regulate Vg production. Together, these coordinately result in substantial reduction of Vg in the fat body, accompanied by blocked oocyte maturation and ovarian growth.

Experimental procedures

Experimental animals

The colony of migratory locusts in the gregarious phase was reared under a photoperiod of 14 light:10 dark and at 30 ± 2 °C as previously described (50). The diet included a continuous supply of wheat bran with fresh wheat seedlings provided once daily. The JH-deprived adult females were achieved by inactivation of corpora allata with topical application of 500 μg (100 μg/μl dissolved in acetone) precocene III (Sigma) per locust to the dorsal neck membrane within 12 h post-eclosion. To restore JH activity, *s*-(+)-methoprene (Santa Cruz Biotechnology) was topically applied at 150 μg (30 μg/μl dissolved in acetone) per locust 10 days post-precocene treatment. Topical application of acetone (5 μl per locust) alone was used as the solvent control (50).

Phylogenetic analysis

The coding sequences of *Grp78* genes available in the GenBank™ database of NCBI were collected. Multiple sequence alignments were performed with ClustalW and the phylogenetic tree was constructed using MAGA6 with the Neighbor Joining method.

RNA isolation and qRT-PCR

Total RNA from locust tissues and *Drosophila* S2 cells was extracted with TRIzol reagent (Invitrogen). First-strand cDNA was reverse-transcribed using FastQuant RT Kit with gDNase (Tiangen). qRT-PCR was performed on the Mx3005P detection system (Agilent) using SuperReal PreMix Plus (SYBR Green) Kit (Tiangen), initiated at 95 °C for 2 min, then 40 cycles at 95 °C for 20 s followed by 58 °C for 20 s and 68 °C for 1 min. The relative expression levels were calculated using the $2^{-\Delta\Delta Ct}$ method, with locust Ribosomal protein 49 (Rp49) and *Drosophila* β-actin as the internal controls. Melting curve analysis was conducted to verify the specificity of amplification. The qRT-PCR products were sequenced for the confirmation of primer specificity. For absolute quantification (87), qRT-PCR products of *Grp78-1* and *Grp78-2* were separately cloned into pGM-T vector (Tiangen), confirmed by sequencing, and serially diluted to serve as the reference standards. *Grp78-1* and *Grp78-2* transcripts in the fat body were quantified with the standard curves derived from the calibration experiments by plotting the natural log of threshold cycle (C_t) against that of serially diluted recombinant plasmids. Primers used for qRT-PCR are listed in Table 1.

RNA interference (RNAi)

cDNA templates were amplified by PCR, cloned into pGM-T easy vector (Tiangen), and confirmed by sequencing. Double-stranded RNA (dsRNA) was then synthesized by *in vitro* transcription with T7 RiboMAX Express System (Promega) following the manufacturer's instruction. For RNAi in locusts, adult females within 12 h after eclosion were intra-abdominally

Table 1
Primers used for qRT-PCR or RNAi

	Gene	Forward primer	Reverse primer
qRT-PCR	*Met*	CCACTTACAGGCTTGCTA	GCCCTTCTTCACCTTCTT
	Mcm4	GGCGAATTGCGGAACCTACC	GCAGGCATATCATCAGGCGATT
	Mcm7	ACGAGTTTGACAAGATGGCTGAC	ACGACCATAGGCTGGATTTGC
	Grp78-1	GGGGACACTCATTTGGGTG	TTGCTTTTTCTACTTCACGGC
	Grp78-2	TGTTAGTAGGTGGAAGCACAAGGA	GCACAGCAGCACCATATACAACT
	Ire1	TTCTTCTGGGCGAGCACTAAGT	ACAGCAACCAGGCCACTCTC
	Grp94	CACTTCTGCCCAGGATCTCAAT	GCTTGTCATCATTGTGCTTGGT
	PDI	GACAACTCTCCACGGCGGAA	GGTAGACTGTACGGAAGCTGGT
	Grp170	AGACCTTGACCATCTTCCTGAACA	GTGCGTGTCCTTGTGCTTGG
	VgA	CCCACAAGAAGCACAGAACG	TTGGTCGCCATCAACAGAAG
	Rp49	CGTAAACCGAAGGGAATTGA	GAAGAAACTGCATGGGCAAT
	DmMet	CGTCCTTAGATTCGCCACCC	GAGGCAGACATACCCGTTCC
	DmGce	CTCAGTCCCTTCACCTTCAT	ACCTTGTTCGTCTCCTTGTC
	DmTai	AGCGATGTAAAGCCCGAGA	AAAGCAGCATTCCACCCAC
	Dmβ-actin	ACTTCTGCTGGAAGGTGGAC	ATCCGCAAGGATCTGTATGC
RNAi	*Grp78-1*	TATAACCTGCGAACGAGTA	CACTAGGAATGCAATACAGA
	Grp78-2	GTTCTAGTGAGGATGATGAC	TTCAGATATGTAGAGCTAAG
	Grp78	AAGGACAACCATCTGCTAGGAA	GGCTGAACCACATCTTCTAACTC
	Met	TTAGGGCAGCATCAGAAAG	TCGTCGGGAGGAAGTGTAT
	Mcm4	CGCCGTGAAAGAGGTGAAGAAG	AAGCAGGTGGAACTGACTGATGA
	Mcm7	GGAACAGCAGACCATTACCATT	ACATCAGCCAGCCTCAGAC
	Ire1	CGAAGATCACCAACACCGATT	GTCCTTCCAATGAGCACAGATT
	GFP	CACAAGTTCAGCGTGTCCG	GTTCACCTTGATGCCGTTC
	DmMet	CTGCCAACTATCCGATTGTCTC	CTCTCGCCGTAGTCACTGTT
	DmTai	AGCATCAGCACCAGCATCA	GTCGTTGTCGTAGAGTTGTTGT

injected with 15 μg of dsRNA (5 μg/μl dissolved in nuclease-free ddH_2O) and boosted on day 5. For RNAi in S2 cells, *Drosophila Met* (FlyBase: FBpp0073368) and *Tai* (FlyBase: FBpp0292873) dsRNA (38 nM) were transfected into S2 cells using Lipofectamine 2000 (Invitrogen) for 48 h. In JH rescue experiments, 150 μg of methoprene (dissolved in 5 μl of acetone) or 5 μl of acetone (solvent control) was applied to dsGrp78-treated locusts on day 6, and the effects were examined on day 8. GFP dsRNA was used as the mock control. Primers for dsRNA synthesis are included in Table 1.

Vg antibody preparation

A 396-bp cDNA fragment coding for a 132-aa peptide (forward primer, 5′-TACTCAGAATTCCCCGACTACGTTCAACGATT-3′; reverse primer: 5′-TACTCACTCGAGTCAATGATGCTCTTTACTGCGG-3′) of locust VgA was cloned into pET-30a-His and confirmed by sequencing. The recombinant VgA peptide was purified by Ni2-His affinity column and examined by SDS-PAGE. Polyclonal anti-VgA antibody was raised in rabbits using the VgA peptide mixed with Freund's complete adjuvant (Sigma) to form a stable emulsion for immunization. The rabbit was injected subcutaneously at 4 sites, and boosted once a week for a total of 4 times. The antiserum specificity was verified by Western blot analysis as described (see Fig. 4*d* and its legend).

Western blot analysis and immunoprecipitation

Total proteins from the fat body and ovary of 6-day-old adult female locusts were collected using the ice-cold lysis buffer containing 50 mM Tris-HCl, pH 7.5, 150 mM NaCl, 2 mM EDTA, 1 mM DTT, 1% Nonidet P-40, 1 mM PMSF, 1 mM NaF, and a protease inhibitor mixture (Roche Applied Science). Lysates were cleared by centrifugation at 14,000 × *g* for 10 min, fractionated on 8% SDS-PAGE, and transferred to PVDF membranes (Millipore). Extracted proteins were quantified by BCA protein assay kit (Pierce). Western blot analysis was performed using the anti-VgA antibody, the corresponding HRP-conjugated secondary antibodies (CWBIO), and an enhanced chemiluminescent reagent (CWBIO). The anti-GAPDH antibody (MBL) was used as the loading control. Bands were imaged by ChemiDoc XRS system (Bio-Rad) and analyzed by ImageJ software.

For the recombinant proteins, locust Met (GenBank™ KF471131; nt 1–3108) and Tai (Tai-A isoform, GenBank™ KU315327; nt 1–1785 plus 4581–4961) cDNA were cloned into pAc5.1/FLAG and pAc5.1/V5 vectors (Invitrogen), respectively (52). *Drosophila* S2 cells were transfected with pAc5.1/Flag-Met and/or pAc5.1/V5-Tai using Lipofectamine 2000 (Invitrogen) for 48 h, followed by treatment with 10 μM methoprene for 6 h. Cells were then lysed with the ice-cold lysis buffer and cleared by centrifugation. Western blotting was conducted using anti-FLAG or anti-V5 (MBL) antibody. For immunoprecipitation, the pre-cleared lysates were incubated with anti-V5 antibody for 60 min at 4 °C. The immunocomplexes were then captured with protein A-agarose (Sigma) and eluted in Laemmli sample buffer, followed by Western blotting with anti-FLAG antibody.

Luciferase reporter assay

The promoter region of *Grp78-2* (nt −2068 to −24) was cloned into pGL4.10 vector (Promega) and confirmed by sequencing. To obtain the mutant of the E-box-like motif, the sequence CACGCG was substituted by ACATAT (forward primer, 5′-ACATGTAATTATATGTACGAAAATAGGTTAACTTCCGATGTTAGC-3′; reverse primer: 5′- CTATTTTCGTACATATAATTACATGTTGCAGACGACGATTGCACT-3′) using the Q5 Site-directed Mutagenesis Kit (New England Biolabs) and confirmed by sequencing. S2 cells were pretreated with *Drosophila Met* and *Tai* dsRNA for 48 h, and then transfected with pGL4.10-*Grp78-2*(−2068 to −24) plus pAc5.1/Flag-Met(1–3108) and/or pAc5.1/V5-Tai(1–1785 plus 4581–4961) using Lipofectamine 2000 (Invitrogen). After 48 h,

S2 cells were further treated with 10 μM methoprene for 6 h. The Dual-luciferase Reporter Assay System and a GloMax 96 Microplate Luminometer (Promega) were employed to measure the luciferase activity.

Tissue imaging, cell staining, and confocal microscopy

The ovary and ovariole were imaged with Nikon D7000 camera and Olympus CKX41 microscope. The length of primary oocytes was measured with Image Pro PLUS software. For cell staining, sheath-free ovarioles were fixed in 4% paraformaldehyde, and then permeabilized in 0.3% Triton X-100. F-actin and nuclei were stained with 0.165 μM phalloidin/Alexa Fluor 488 (Invitrogen) and 5 μM Hoechst 33342 (Sigma), respectively. The images were captured with ZEISS LSM 710 confocal microscope and processed with ZEN2012 software (Carl Zeiss).

Apoptosis assay

Apoptosis assays were carried out using *In Situ* Cell Death Detection kit (Roche Applied Science) according to the manufacturer's protocol. Briefly, the fat body sections were fixed in 4% paraformaldehyde for 15 min at room temperature, followed by treatment with proteinase K (10 μg/ml) for 40 min at 37 °C. Nuclei were stained with 5 μM Hoechst 33342 (Sigma). Apoptosis was detected with Terminal dUTP Nick End Labeling (TUNEL) reaction mixture. Images were captured with ZEISS LSM 710 confocal microscope and analyzed with ZEN2012 software (Carl Zeiss).

Data analysis

Statistical analyses were performed using Student's t test or one-way analysis of variance with SPSS20.0 software. Significant difference was considered at $p < 0.05$. Values were reported as mean ± S.E.

Author contributions—S. Z. conceived the study. M. L., D. L., and Z. W. performed the experiments and acquired the data. M. L. and S. Z. analyzed the data and wrote the manuscript. W. G. and L. K. provided technical support.

References

1. Riddiford, L. M. (1994) Cellular and molecular actions of juvenile hormone: I. general considerations and premetamorphic actions. in *Advances in Insect Physiology* (Evans, P. D., ed) pp. 213–274, Academic Press, Orlando, FL
2. Wyatt, G. R., and Davey, K. G. (1996) Cellular and molecular actions of juvenile hormone. II. roles of juvenile hormone in adult insects. in *Advances in Insect Physiology* (Evans, P. D., ed) pp. 213–274, Academic Press, Orlando, FL
3. Jindra, M., Palli, S. R., and Riddiford, L. M. (2013) The juvenile hormone signaling pathway in insect development. *Annu. Rev. Entomol.* **58,** 181–204
4. Jindra, M., Uhlirova, M., Charles, J. P., Smykal, V., and Hill, R. J. (2015) Genetic evidence for function of the bHLH-PAS protein Gce/Met as a juvenile hormone receptor. *PLoS Genet.* **11,** e1005394
5. Charles, J. P., Iwema, T., Epa, V. C., Takaki, K., Rynes, J., and Jindra, M. (2011) Ligand-binding properties of a juvenile hormone receptor, methoprene-tolerant. *Proc. Natl. Acad. Sci. U.S.A.* **108,** 21128–21133
6. Kayukawa, T., Minakuchi, C., Namiki, T., Togawa, T., Yoshiyama, M., Kamimura, M., Mita, K., Imanishi, S., Kiuchi, M., Ishikawa, Y., and Shinoda, T. (2012) Transcriptional regulation of juvenile hormone-mediated induction of Kruppel homolog 1, a repressor of insect metamorphosis. *Proc. Natl. Acad. Sci. U.S.A.* **109,** 11729–11734
7. Li, M., Liu, P., Wiley, J. D., Ojani, R., Bevan, D. R., Li, J., and Zhu, J. (2014) A steroid receptor coactivator acts as the DNA-binding partner of the methoprene-tolerant protein in regulating juvenile hormone response genes. *Mol. Cell. Endocrinol.* **394,** 47–58
8. Cui, Y., Sui, Y., Xu, J., Zhu, F., and Palli, S. R. (2014) Juvenile hormone regulates *Aedes aegypti* Kruppel homolog 1 through a conserved E box motif. *Insect Biochem. Mol. Biol.* **52,** 23–32
9. Belles, X., and Santos, C. G. (2014) The MEKRE93 (Methoprene tolerant-Kruppel homolog 1-E93) pathway in the regulation of insect metamorphosis, and the homology of the pupal stage. *Insect Biochem. Mol. Biol.* **52,** 60–68
10. Ureña, E., Manjón, C., Franch-Marro, X., and Martín, D. (2014) Transcription factor E93 specifies adult metamorphosis in hemimetabolous and holometabolous insects. *Proc. Natl. Acad. Sci. U.S.A.* **111,** 7024–7029
11. Ureña, E., Chafino, S., Manjón, C., Franch-Marro, X., and Martín, D. (2016) The occurrence of the holometabolous pupal stage requires the interaction between E93, Kruppel-Homolog 1 and Broad-Complex. *PLoS Genet.* **12,** e1006020
12. Liu, X., Dai, F., Guo, E., Li, K., Ma, L., Tian, L., Cao, Y., Zhang, G., Palli, S. R., and Li, S. (2015) 20-hydroxyecdysone (20E) primary response gene *E93* modulates 20E signaling to promote *Bombyx* larval-pupal metamorphosis. *J. Biol. Chem.* **290,** 27370–27383
13. Raikhel, A. S., Kokoza, V. A., Zhu, J., Martin, D., Wang, S. F., Li, C., Sun, G., Ahmed, A., Dittmer, N., and Attardo, G. (2002) Molecular biology of mosquito vitellogenesis: from basic studies to genetic engineering of antipathogen immunity. *Insect Biochem. Mol. Biol.* **32,** 1275–1286
14. Shin, S. W., Zou, Z., Saha, T. T., and Raikhel, A. S. (2012) bHLH-PAS heterodimer of methoprene-tolerant and cycle mediates circadian expression of juvenile hormone-induced mosquito genes. *Proc. Natl. Acad. Sci. U.S.A.* **109,** 16576–16581
15. Raikhel, A. S., Brown, M. R., and Bellés, X. (2005) Hormonal control of reproductive processes. in *Comprehensive Molecular Insect Science* (Gilbert, L. I., ed) pp. 433–491, Elsevier, Amsterdam
16. Riddiford, L. M. (2012) How does juvenile hormone control insect metamorphosis and reproduction? *Gen. Comp. Endocrinol.* **179,** 477–484
17. Bellés, X. (2005) Vitellogenesis directed by juvenile hormone. in *Reproductive Biology of Invertebrates* (Raikhel, A. S., and Sappington, T. W., eds) pp. 157–198, Science Publishers, Enfield, Plymouth, UK
18. Cruz, J., Martín, D., Pascual, N., Maestro, J. L., Piulachs, M. D., and Bellés, X. (2003) Quantity does matter. Juvenile hormone and the onset of vitellogenesis in the German cockroach. *Insect Biochem. Mol. Biol.* **33,** 1219–1225
19. Smykal, V., Bajgar, A., Provaznik, J., Fexova, S., Buricova, M., Takaki, K., Hodkova, M., Jindra, M., and Dolezel, D. (2014) Juvenile hormone signaling during reproduction and development of the linden bug, *Pyrrhocoris apterus. Insect Biochem. Mol. Biol.* **45,** 69–76
20. Marchal, E., Hult, E. F., Huang, J., Pang, Z., Stay, B., and Tobe, S. S. (2014) Methoprene-tolerant (Met) knockdown in the adult female cockroach, *Diploptera punctata* completely inhibits ovarian development. *PLoS ONE* **9,** e106737
21. Raikhel, A. S., and Dhadialla, T. S. (1992) Accumulation of york proteins in insect oocytes. *Annu. Rev. Entomol.* **37,** 217–251
22. Haas, I. G. (1994) BiP (GRP78), an essential hsp70 resident protein in the endoplasmic reticulum. *Experientia* **50,** 1012–1020
23. Haas, I. G., and Wabl, M. (1983) Immunoglobulin heavy chain binding protein. *Nature* **306,** 387–389
24. Gething, M. J. (1999) Role and regulation of the ER chaperone BiP. *Semin. Cell Dev. Biol.* **10,** 465–472
25. Rutkowski, D. T., and Kaufman, R. J. (2004) A trip to the ER: coping with stress. *Trends Cell Biol.* **14,** 20–28
26. Schröder, M., and Kaufman, R. J. (2005) The mammalian unfolded protein response. *Annu. Rev. Biochem.* **74,** 739–789
27. Ron, D., and Walter, P. (2007) Signal integration in the endoplasmic reticulum unfolded protein response. *Nat. Rev. Mol. Cell Biol.* **8,** 519–529
28. Walter, P., and Ron, D. (2011) The unfolded protein response: from stress pathway to homeostatic regulation. *Science* **334,** 1081–1086

29. Lee, J., and Ozcan, U. (2014) Unfolded protein response signaling and metabolic diseases. *J. Biol. Chem.* **289,** 1203–1211
30. Hetz, C. (2012) The unfolded protein response: controlling cell fate decisions under ER stress and beyond. *Nat. Rev. Mol. Cell Biol.* **13,** 89–102
31. Ozcan, L., Ergin, A. S., Lu, A., Chung, J., Sarkar, S., Nie, D., Myers, M. G., Jr., and Ozcan, U. (2009) Endoplasmic reticulum stress plays a central role in development of leptin resistance. *Cell Metab.* **9,** 35–51
32. Ozcan, U., Cao, Q., Yilmaz, E., Lee, A. H., Iwakoshi, N. N., Ozdelen, E., Tuncman, G., Görgün, C., Glimcher, L. H., and Hotamisligil, G. S. (2004) Endoplasmic reticulum stress links obesity, insulin action, and type 2 diabetes. *Science* **306,** 457–461
33. Clegg, D. J., Gotoh, K., Kemp, C., Wortman, M. D., Benoit, S. C., Brown, L. M., D'Alessio, D., Tso, P., Seeley, R. J., and Woods, S. C. (2011) Consumption of a high-fat diet induces central insulin resistance independent of adiposity. *Physiol. Behav.* **103,** 10–16
34. Biddinger, S. B., and Kahn, C. R. (2006) From mice to men: insights into the insulin resistance syndromes. *Annu. Rev. Physiol.* **68,** 123–158
35. Bochkis, I. M., Rubins, N. E., White, P., Furth, E. E., Friedman, J. R., and Kaestner, K. H. (2008) Hepatocyte-specific ablation of *Foxa2* alters bile acid homeostasis and results in endoplasmic reticulum stress. *Nat. Med.* **14,** 828–836
36. Tamaki, N., Hatano, E., Taura, K., Tada, M., Kodama, Y., Nitta, T., Iwaisako, K., Seo, S., Nakajima, A., Ikai, I., and Uemoto, S. (2008) CHOP deficiency attenuates cholestasis-induced liver fibrosis by reduction of hepatocyte injury. *Am. J. Physiol. Gastrointest. Liver Physiol.* **294,** G498–G505
37. Glembotski, C. C. (2008) The role of the unfolded protein response in the heart. *J. Mol. Cell Cardiol.* **44,** 453–459
38. Thorp, E., Li, G., Seimon, T. A., Kuriakose, G., Ron, D., and Tabas, I. (2009) Reduced apoptosis and plaque necrosis in advanced atherosclerotic lesions of $Apoe^{-/-}$ and $Ldlr^{-/-}$ mice lacking CHOP. *Cell Metab.* **9,** 474–481
39. Matus, S., Glimcher, L. H., and Hetz, C. (2011) Protein folding stress in neurodegenerative diseases: a glimpse into the ER. *Curr. Opin. Cell Biol.* **23,** 239–252
40. Mercado, G., Valdés, P., and Hetz, C. (2013) An ERcentric view of Parkinson's disease. *Trends Mol. Med.* **19,** 165–175
41. Roussel, B. D., Kruppa, A. J., Miranda, E., Crowther, D. C., Lomas, D. A., and Marciniak, S. J. (2013) Endoplasmic reticulum dysfunction in neurological disease. *Lancet Neurol.* **12,** 105–118
42. Garrett, W. S., Gordon, J. I., and Glimcher, L. H. (2010) Homeostasis and inflammation in the intestine. *Cell* **140,** 859–870
43. Kaser, A., Flak, M. B., Tomczak, M. F., and Blumberg, R. S. (2011) The unfolded protein response and its role in intestinal homeostasis and inflammation. *Exp. Cell Res.* **317,** 2772–2779
44. Moenner, M., Pluquet, O., Bouchecareilh, M., and Chevet, E. (2007) Integrated endoplasmic reticulum stress responses in cancer. *Cancer Res.* **67,** 10631–10634
45. Müller, H., Schmidt, D., Steinbrink, S., Mirgorodskaya, E., Lehmann, V., Habermann, K., Dreher, F., Gustavsson, N., Kessler, T., Lehrach, H., Herwig, R., Gobom, J., Ploubidou, A., Boutros, M., and Lange, B. M. (2010) Proteomic and functional analysis of the mitotic *Drosophila* centrosome. *EMBO J.* **29,** 3344–3357
46. Ugrankar, R., Berglund, E., Akdemir, F., Tran, C., Kim, M. S., Noh, J., Schneider, R., Ebert, B., and Graff, J. M. (2015) *Drosophila* glucome screening identifies Ck1α as a regulator of mammalian glucose metabolism. *Nat. Commun.* **6,** 7102
47. Dorner, S., Lum, L., Kim, M., Paro, R., Beachy, P. A., and Green, R. (2006) A genomewide screen for components of the RNAi pathway in *Drosophila* cultured cells. *Proc. Natl. Acad. Sci. U.S.A.* **103,** 11880–11885
48. Naidoo, N., Casiano, V., Cater, J., Zimmerman, J., and Pack, A. I. (2007) A role for the molecular chaperone protein BiP/GRP78 in *Drosophila* sleep homeostasis. *Sleep* **30,** 557–565
49. Zhang, G., Storey, J. M., and Storey, K. B. (2011) Chaperone proteins and winter survival by a freeze tolerant insect. *J. Insect Physiol.* **57,** 1115–1122
50. Guo, W., Wu, Z., Song, J., Jiang, F., Wang, Z., Deng, S., Walker, V. K., and Zhou, S. (2014) Juvenile hormone-receptor complex acts on *Mcm4* and *Mcm7* to promote polyploidy and vitellogenesis in the migratory locust. *PLoS Genet.* **10,** e1004702
51. Wu, Z., Guo, W., Xie, Y., and Zhou, S. (2016) Juvenile hormone activates the transcription of cell-division-cycle 6 (*Cdc6*) for polyploidy-dependent insect vitellogenesis and oogenesis. *J. Biol. Chem.* **291,** 5418–5427
52. Wang, Z., Yang, L., Song, J., Kang, L., and Zhou, S. (2017) An isoform of Taiman that contains a PRD-repeat motif is indispensable for transducing the vitellogenic juvenile hormone signal in *Locusta migratoria*. *Insect Biochem. Mol. Biol.* **82,** 31–40
53. Wang, X., Fang, X., Yang, P., Jiang, X., Jiang, F., Zhao, D., Li, B., Cui, F., Wei, J., Ma, C., Wang, Y., He, J., Luo, Y., Wang, Z., Guo, X., *et al.* (2014) The locust genome provides insight into swarm formation and long-distance flight. *Nat. Commun.* **5,** 2957
54. Dale, J. F., and Tobe, S. S. (1986) Biosynthesis and titre of juvenile hormone during the first gonotrophic cycle in isolated and crowded *Locusta migratoria* females. *J. Insect Physiol.* **32,** 763–769
55. Glinka, A. V., Braun, R. P., Edwards, J. P., and Wyatt, G. R. (1995) The use of a juvenile hormone binding protein for the quantitative assay of juvenile hormone. *Insect Biochem. Mol. Biol.* **25,** 775–781
56. Li, M., Mead, E. A., and Zhu, J. (2011) Heterodimer of two bHLH-PAS proteins mediates juvenile hormone-induced gene expression. *Proc. Natl. Acad. Sci. U.S.A.* **108,** 638–643
57. He, Q., Wen, D., Jia, Q., Cui, C., Wang, J., Palli, S. R., and Li, S. (2014) Heat shock protein 83 (Hsp83) facilitates methoprene-tolerant (Met) nuclear import to modulate juvenile hormone signaling. *J. Biol. Chem.* **289,** 27874–27885
58. Song, J., Wu, Z., Wang, Z., Deng, S., and Zhou, S. (2014) Kruppel-homolog 1 mediates juvenile hormone action to promote vitellogenesis and oocyte maturation in the migratory locust. *Insect Biochem. Mol. Biol.* **52,** 94–101
59. Moore, A. W., Barbel, S., Jan, L. Y., and Jan, Y. N. (2000) A genomewide survey of basic helix-loop-helix factors in *Drosophila*. *Proc. Natl. Acad. Sci. U.S.A.* **97,** 10436–10441
60. Abdou, M. A., He, Q., Wen, D., Zyaan, O., Wang, J., Xu, J., Baumann, A. A., Joseph, J., Wilson, T. G., Li, S., and Wang, J. (2011) *Drosophila* Met and Gce are partially redundant in transducing juvenile hormone action. *Insect Biochem. Mol. Biol.* **41,** 938–945
61. Huebner, E., and Injeyan, H. S. (1980) Patency of the follicular epithelium in *Rhodnius prolixus*: a re-examination of the hormone response and technique refinement. *Can. J. Zool.* **58,** 1617–1625
62. Kusaczuk, M., and Cechowska-Pasko, M. (2013) Molecular chaperone ORP150 in ER stress-related diseases. *Curr. Pharm. Des.* **19,** 2807–2818
63. Lee, A. S. (2014) Glucose-regulated proteins in cancer: molecular mechanisms and therapeutic potential. *Nat. Rev. Cancer* **14,** 263–276
64. Wang, H., Pezeshki, A. M., Yu, X., Guo, C., Subjeck, J. R., and Wang, X. Y. (2014) The endoplasmic reticulum chaperone GRP170: from immunobiology to cancer therapeutics. *Front Oncol.* **4,** 377
65. Kaufman, R. J. (1999) Stress signaling from the lumen of the endoplasmic reticulum: coordination of gene transcriptional and translational controls. *Genes Dev.* **13,** 1211–1233
66. Chen, Y., and Brandizzi, F. (2013) IRE1: ER stress sensor and cell fate executor. *Trends Cell Biol.* **23,** 547–555
67. Gao, Y. Y., Liu, B. Q., Du, Z. X., Zhang, H. Y., Niu, X. F., and Wang, H. Q. (2010) Implication of oxygen-regulated protein 150 (ORP150) in apoptosis induced by proteasome inhibitors in human thyroid cancer cells. *J. Clin. Endocrinol. Metab.* **95,** E319–E326
68. Namba, T., Hoshino, T., Tanaka, K., Tsutsumi, S., Ishihara, T., Mima, S., Suzuki, K., Ogawa, S., and Mizushima, T. (2007) Up-regulation of 150-kDa oxygen-regulated protein by celecoxib in human gastric carcinoma cells. *Mol. Pharmacol.* **71,** 860–870
69. Kaneda, S., Yura, T., and Yanagi, H. (2000) Production of three distinct mRNAs of 150 kDa oxygen-regulated protein (ORP150) by alternative promoters: preferential induction of one species under stress conditions. *J. Biochem.* **128,** 529–538
70. Han, D., Lerner, A. G., Vande Walle, L., Upton, J. P., Xu, W., Hagen, A., Backes, B. J., Oakes, S. A., and Papa, F. R. (2009) IRE1α kinase activation modes control alternate endoribonuclease outputs to determine divergent cell fates. *Cell* **138,** 562–575

71. Zhang, K., and Kaufman, R. J. (2006) The unfolded protein response: a stress signaling pathway critical for health and disease. *Neurology* **66,** S102–S109
72. Kleizen, B., and Braakman, I. (2004) Protein folding and quality control in the endoplasmic reticulum. *Curr. Opin. Cell Biol.* **16,** 343–349
73. Fu, Y., Li, J., and Lee, A. S. (2007) GRP78/BiP inhibits endoplasmic reticulum BIK and protects human breast cancer cells against estrogen starvation-induced apoptosis. *Cancer Res.* **67,** 3734–3740
74. Pyrko, P., Schönthal, A. H., Hofman, F. M., Chen, T. C., and Lee, A. S. (2007) The unfolded protein response regulator GRP78/BiP as a novel target for increasing chemosensitivity in malignant gliomas. *Cancer Res.* **67,** 9809–9816
75. Shu, C. W., Sun, F. C., Cho, J. H., Lin, C. C., Liu, P. F., Chen, P. Y., Chang, M. D., Fu, H. W., and Lai, Y. K. (2008) GRP78 and Raf-1 cooperatively confer resistance to endoplasmic reticulum stress-induced apoptosis. *J. Cell. Physiol.* **215,** 627–635
76. Virrey, J. J., Dong, D., Stiles, C., Patterson, J. B., Pen, L., Ni, M., Schönthal, A. H., Chen, T. C., Hofman, F. M., and Lee, A. S. (2008) Stress chaperone GRP78/BiP confers chemoresistance to tumor-associated endothelial cells. *Mol. Cancer Res.* **6,** 1268–1275
77. Xu, D., Perez, R. E., Rezaiekhaligh, M. H., Bourdi, M., and Truog, W. E. (2009) Knockdown of ERp57 increases BiP/GRP78 induction and protects against hyperoxia and tunicamycin-induced apoptosis. *Am. J. Physiol. Lung Cell Mol. Physiol.* **297,** L44–L51
78. Ellgaard, L., and Helenius, A. (2003) Quality control in the endoplasmic reticulum. *Nat. Rev. Mol. Cell Biol.* **4,** 181–191
79. Xu, C., Bailly-Maitre, B., and Reed, J. C. (2005) Endoplasmic reticulum stress: cell life and death decisions. *J. Clin. Invest.* **115,** 2656–2664
80. Back, S. H., Scheuner, D., Han, J., Song, B., Ribick, M., Wang, J., Gildersleeve, R. D., Pennathur, S., and Kaufman, R. J. (2009) Translation attenuation through eIF2α phosphorylation prevents oxidative stress and maintains the differentiated state in beta cells. *Cell Metab.* **10,** 13–26
81. Nair, K. K., Chen, T. T., and Wyatt, G. R. (1981) Juvenile hormone-stimulated polyploidy in adult locust fat body. *Dev. Biol.* **81,** 356–360
82. Oishi, M., Locke, J., and Wyatt, G. R. (1985) The ribosomal RNA genes of *Locusta migratoria*: copy number and evidence for underreplication in a polyploid tissue. *Can. J. Biochem. Cell Biol.* **63,** 1064–1070
83. Brewer, J. W., Cleveland, J. L., and Hendershot, L. M. (1997) A pathway distinct from the mammalian unfolded protein response regulates expression of endoplasmic reticulum chaperones in non-stressed cells. *EMBO J.* **16,** 7207–7216
84. Pfaffenbach, K. T., Pong, M., Morgan, T. E., Wang, H., Ott, K., Zhou, B., Longo, V. D., and Lee, A. S. (2012) GRP78/BiP is a novel downstream target of IGF-1 receptor mediated signaling. *J. Cell. Physiol.* **227,** 3803–3811
85. Iwamune, M., Nakamura, K., Kitahara, Y., and Minegishi, T. (2014) MicroRNA-376a regulates *79*-kilodalton glucose-regulated protein expression in rat granulosa cells. *PLoS ONE* **9,** e108997
86. Thon, M., Hosoi, T., Yoshii, M., and Ozawa, K. (2014) Leptin induced GRP78 expression through the PI3K-mTOR pathway in neuronal cells. *Sci. Rep.* **4,** 7096
87. Whelan, J. A., Russell, N. B., and Whelan, M. A. (2003) A method for the absolute quantification of cDNA using real-time PCR. *J. Immunol. Methods* **278,** 261–269
88. Zou, Z., Saha, T. T., Roy, S., Shin, S. W., Backman, T. W., Girke, T., White, K. P., and Raikhel, A. S. (2013) Juvenile hormone and its receptor, methoprene-tolerant, control the dynamics of mosquito gene expression. *Proc. Natl. Acad. Sci. U.S.A.* **110,** E2173–E2181